Human Molecular Genetics, 2015, Vol. 24, No. 1 **251–264**
doi:10.1093/hmg/ddu443
Advance Access published on August 28, 2014

NKX2-5, a modifier of skeletal muscle pathology due to RNA toxicity

Jordan T. Gladman†, Ramesh S. Yadava†, Mahua Mandal, Qing Yu, Yun K. Kim and Mani S. Mahadevan*

Department of Pathology, University of Virginia, Charlottesville, VA 22908, USA

Received June 11, 2014; Revised July 30, 2014; Accepted August 26, 2014

RNA toxicity is implicated in a number of disorders; especially those associated with expanded repeat sequences, such as myotonic dystrophy (DM1). Previously, we have shown increased *NKX2-5* expression in RNA toxicity associated with DM1. Here, we investigate the relationship between NKX2-5 expression and muscle pathology due to RNA toxicity. In skeletal muscle from mice with RNA toxicity and individuals with DM1, expression of *Nkx2-5* or *NKX2-5* and its downstream targets are significantly correlated with severity of histopathology. Using C2C12 myoblasts, we show that over-expression of NKX2-5 or mutant *DMPK* 3′UTR results in myogenic differentiation defects, which can be rescued by knockdown of *Nkx2-5*, despite continued toxic RNA expression. Furthermore, in a mouse model of NKX2-5 over-expression, we find defects in muscle regeneration after induced damage, similar to those seen in mice with RNA toxicity. Using mouse models of *Nkx2-5* over-expression and depletion, we find that NKX2-5 levels modify disease phenotypes in mice with RNA toxicity.

INTRODUCTION

Myotonic dystrophy (DM1) is an autosomal dominant disorder caused by an expanded $(CTG)_n$ tract in the 3′ untranslated region (3′UTR) of the dystrophia myotonica protein kinase (*DMPK*) gene resulting in nuclear entrapment of the 'toxic' mutant RNA and interacting RNA-binding proteins (1–3). DM1 is a multi-systemic disorder characterized by progressive muscle wasting, and the first example of a disease caused by RNA toxicity. Mutant DMPK mRNAs form nuclear aggregates and are thought to mediate adverse effects by affecting interactions with or altered activity of RNA splicing factors such as Muscleblind-like 1(MBNL1) and CUG-binding protein 1 (CELF1), resulting in aberrant splicing of various target mRNAs in affected tissues.

The major debilitating factor in DM1 is muscle wasting. Previously, we found that expression of the mutant DMPK 3′UTR mRNA in C2C12 mouse myoblasts results in defective myogenic differentiation (4–7). Several other groups have also reported differentiation defects (8–11) or in one case, normal differentiation but abnormal apoptosis (12) using primary myoblasts from DM1 patients. Using two separate inducible-reversible transgenic mouse lines of RNA toxicity, we demonstrated that over-expression of *DMPK*-3′UTR mRNAs reproduced many disease features including characteristic histologic abnormalities, severe muscle pathology, CELF1 up-regulation, RNA splicing defects, myotonia, cardiac conduction defects and showed that they are potentially reversible (13). Additionally, we have shown that the phenotype in these mice can be modulated by altering their genotype or doxycline dosage, or CELF1 levels (14). Also we have shown that the transgene transcript in these mice interacts with MBNL1 (15) and that over-expression of MBNL1 can modulate phenotypes such as altered splicing and myotonia in these mice, similar to what has been demonstrated in other mouse models of RNA toxicity (16). Unexpectedly, we also found induction of NKX2-5 in skeletal muscles, a result that was confirmed in skeletal muscles from DM1 patients (17).

During mouse development, NKX2-5, a transcription factor, is detected in cardiac progenitors and pharyngeal endoderm as early as 7.5-day post-coitum (18,19) and is also detected in a subset of cranial skeletal muscles, spleen, stomach, liver, tongue and anterior larynx (20). However, in adult mice and humans, its expression is primarily restricted to cardiac tissues; it is not expressed in skeletal muscles. The homozygous deletion of Nkx2-5 in mice is lethal at early stages of cardiac development, and therefore, it has been difficult to study the function of NKX2-5 in the development of other organs as

*To whom correspondence should be addressed. Tel: +1 4342434816; Fax: +1 4349241545; Email: mahadevan@virginia.edu
†These authors contributed equally to this work.

well as in the differentiation and maturation of cardiac myocytes (21). The effects of NKX2-5 in skeletal muscle have not been studied thus far. Here, we sought to understand the role of increased NKX2-5 levels in skeletal muscle pathology due to RNA toxicity using myoblast cell culture models, transgenic mouse models of RNA toxicity and transgenic and knockout mouse models of NKX2.5.

RESULTS

NKX2-5 mRNA levels correlate with muscle histopathology in mice and humans

We analyzed the skeletal muscles from our doxycycline inducible mouse models of RNA toxicity where NKX2-5 expression is induced in multiple transgenic lines (5–313 and 5–336) (17). In these mice, over-expression of a mRNA containing a normal *DMPK* 3′UTR with only $(CUG)_5$ mimics the toxicity of the mutant *DMPK* transcript. We can induce differing levels of DM1 pathology in these mice by altering their genotype (hemizygous or homozygous for the transgene locus) and the dosage of doxycycline. DM1 histopathology is typically characterized by progressive myopathic changes ranging from central nucleation, fiber atrophy and damage, leading eventually to fibrosis and fatty infiltration. Figure 1A and Supplementary Material, Figure S1 depict typical findings with hematoxylin and eosin (H&E)-stained muscle sections in this model. A quantitative histopathology scale was applied by an observer blinded to the genotype and disease status of the mice ($n = 34$) to determine the extent of the histopathology. Next, we analyzed the expression of *Nkx2-5* mRNA by reverse-transcription polymerase chain reaction (RT-PCR) in the same muscles and determined if there was any correlation between *Nkx2-5* expression and histopathology. As shown in Figure 1B, *Nkx2-5* mRNA expression is higher in the muscles with moderate to severe pathology ($n = 17$, grades 2–3) as compared with muscles with mild pathology ($n = 12$, grade 1), and it is undetectable in normal muscles ($n = 5$, grade 0). By quantitative RT-PCR (qRT-PCR), we observed a significant correlation between *Nkx2-5* transcript levels and severity of muscle histopathology ($P < 0.05$, ANOVA) (Fig. 1C). We also assessed the expression of *Nppa* [atrial natriuretic peptide (ANP)] and *Nppb* [brain natriuretic peptide (BNP)] by RT-PCR (Fig. 1B) and *Gata4* expression by qRT-PCR (Supplementary Material, Fig. S2) and found increased expression of all three transcripts in muscles with severe histopathology as compared with mild histopathology. Additionally, we observed a significantly higher level of *Gata4* mRNA in severely affected muscles as compared with mildly affected muscles ($P < 0.041$), or unaffected muscles ($P < 0.002$) (Supplementary Material, Fig. S2). In normal muscles, the expression of these mRNAs was either not detectable or extremely low.

To determine the specificity of *Nkx2-5* mRNA expression, we checked by RT-PCR, the expression of *Nkx2-5* and one of its downstream targets, *Nppb*, in skeletal muscles of several other mouse models. The HSA-LR mouse (a widely used mouse model for DM1) expresses a skeletal muscle actin transgene with a $(CTG)_{250}$ tract in its 3′UTR (22); the *Clcn1*$^{-/-}$ mouse is a model of myotonia caused by the absence of chloride channel (23); the MDX mouse is a model of Duchenne muscular dystrophy (DMD) (24) and the green fluorescent protein (GFP) mouse expresses GFP widely (25) and was used to control for effects of GFP. Notably, despite the presence of obvious myopathy and histopathology in the HSA-LR, *Clcn1*$^{-/-}$ and the MDX mice (Supplementary Material, Fig. S1), we found that *Nkx2-5* and *Nppb* mRNAs are present only in the mice with *DMPK* 3′UTR mRNA toxicity (Fig. 1D). This suggests that the results are not due to a non-specific response to myopathy. Similarly, it is not a response to myotonia, because both the HSA-LR and the *Clcn*$^{-/-}$ mice have extensive myotonia. Nor is it a response to GFP expression. Additionally we examined skeletal muscle from Mbnl1$^{-/-}$ and a Mbnl1$^{-/-}$/Mbnl2$^{+/-}$ mice (26) and found no expression of *Nkx2-5* (data not shown).

To assess possible relevance to DM1, we analyzed skeletal muscle samples from DM1 patients by western blotting, qRT-PCR and immunofluorescence. We observed variable *NKX2-5* expression and assessed if expression of *NKX2-5* correlated with the severity of muscle pathology, as in our mouse models. Figure 1E and Supplementary Material, Figure S3 depict representative H&E pictures of variably affected muscles from DM1 patients, and a sample from a severely affected DMD patient. Compared with mildly affected muscles from DM1 patients, western blotting showed that NKX2-5 protein levels were approximately 5-fold higher in muscles with severe histopathology (Fig. 1F, upper panel). In contrast, muscles from patients with DMD or other muscular dystrophies, and normal muscles did not express NKX2-5. Samples from two DM2 patients were also analyzed, but the results showed no consistent evidence of increased NKX2-5 expression. We found similar results with RT-PCR (Fig. 1F, lower panel). Although sample numbers were limited, we found a clear and statistically significant correlation ($P < 0.05$, ANOVA) between histopathology grade and qRT-PCR for *NKX2-5* expression in DM1 samples (Fig. 1G). Indirect immunofluorescence for NKX2-5 showed expression in skeletal muscles from DM1 patients (Fig. 1H). These results support the validity of the findings from our mouse model.

We also analyzed the expression of NKX2-5 target genes (*NPPA* and *NPPB*) (ANP and BNP) and other cardiac transcription factors (*GATA4*, *TBX5*, and *TBX20*) (Supplementary Material, Fig. S4). These genes were not expressed at appreciable levels in unaffected human skeletal muscles. We found increased levels of *NPPA*, *NPPB*, G*ATA4*, *TBX20* and *TBX5* mRNA only in severely affected DM1 muscles. The expression of *TBX5* was also seen in DMD muscles. These results demonstrate that the expression of NKX2-5 downstream targets also seem to correlate with muscle histopathology in DM1.

Nkx2-5 contributes to myogenic differentiation defects in a C2C12 cell culture model of RNA toxicity

Previously, we found that expression of the mutant *DMPK* 3′UTR mRNA in C2C12 mouse myoblasts results in defective myogenic differentiation (4–7). Using qRT-PCR, we found that *Nkx2-5* mRNA levels were clearly induced, more than 20-fold in cells expressing the *DMPK* 3′UTR $(CTG)_{200}$ mRNA (termed GFP-200 or DM200), and increased about 3.8-fold in the cells expressing the *DMPK* 3′UTR $(CTG)_5$ mRNA (termed GFP-5 or DM5), as compared with wild-type C2C12 cells (Fig. 2A). *Nkx2-5* mRNA was greater in the GFP-200 cells despite lower levels of *DMPK* 3′UTR mRNA as compared

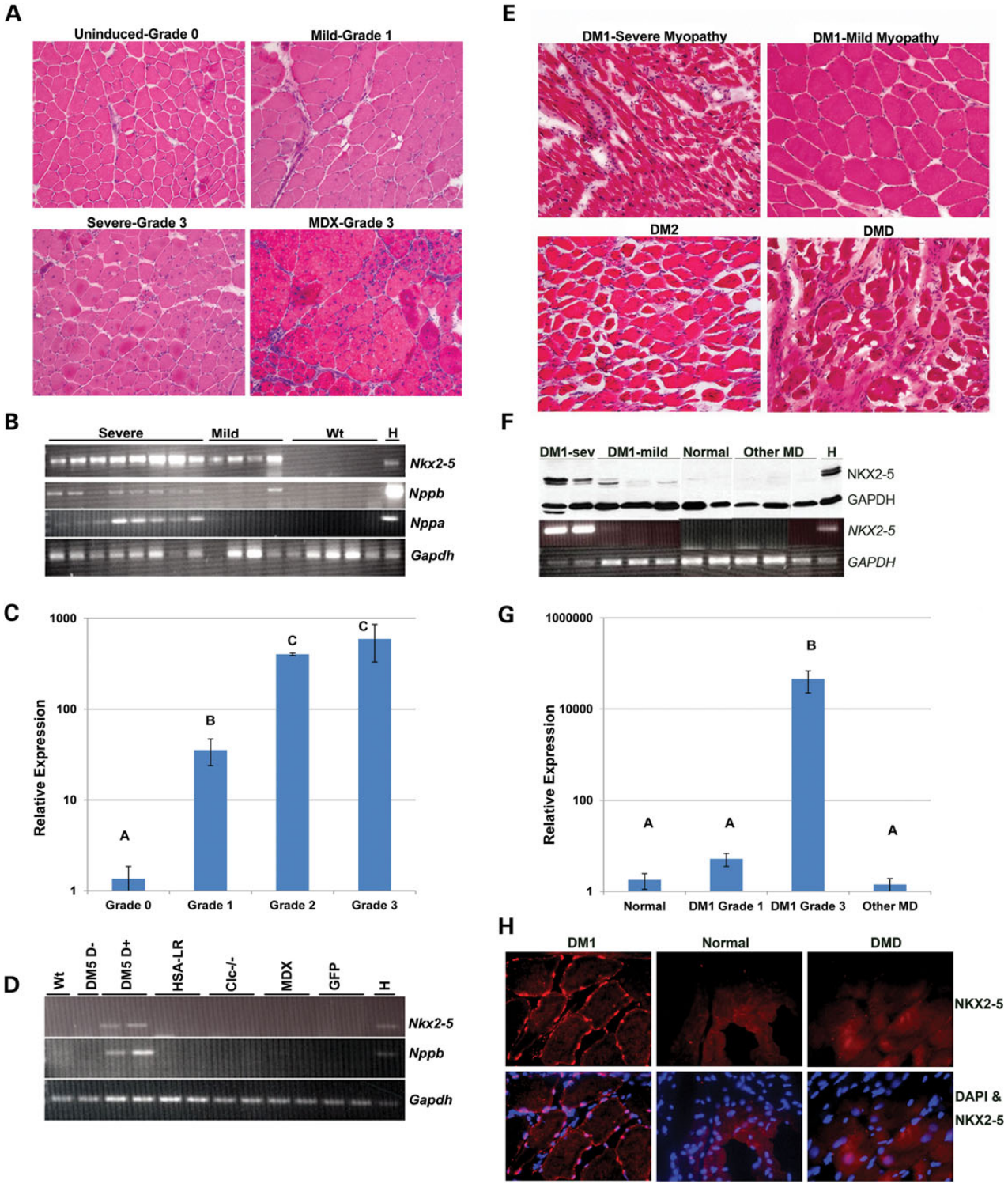

Figure 1. Expression of *Nkx2-5* is correlated with severity of muscle pathology. (**A**) H&E-stained sections of skeletal muscle showing varying severity of histopathology in the DM5-313-D+ mice and *Mdx* mouse; ×200 magnification. (**B**) RT-PCR of *Nkx2-5* and its transcriptional targets (*Nppb, Nppa*) show increased expression in severely affected muscles; a heart extract (H)-positive control; *Gapdh*-loading control. (**C**) qRT-PCR shows clear correlation between muscle histopathology severity and *Nkx2-5* mRNA levels; mean ± SEM. Groups A, B and C are significantly different from each other ($P < 0.05$) (one-way ANOVA with Tukey's LSD multiple comparison). (**D**) RT-PCR shows *Nkx2-5* and *Nppb* mRNA expression in skeletal muscle is specific to *DMPK* 3′UTR mRNA toxicity. Mice genotypes as indicated; a heart extract (H)-positive control; Ga*pdh*-loading control. (**E**) H&E-stained cross-sections of human skeletal muscles showing varying severity of histopathology at ×200 magnification; disease state as indicated. (**F**) Western blot (upper panel) and RT-PCR (lower panel) show increased expression of NKX2-5 and *NKX2-5* mRNA, respectively, in severely affected DM1 skeletal muscles (lanes 1 and 2) as compared with other indicated conditions; a heart extract (H)-positive control; GAPDH- loading control. (**G**) qRT-PCR demonstrates clear correlation between the severity of muscle histopathology and *NKX2-5* mRNA levels in DM1 tissues; statistical analysis as per (C). (**H**) Immunofluorescence for NKX2-5 shows expression in DM1 skeletal muscles but not in other indicated conditions.

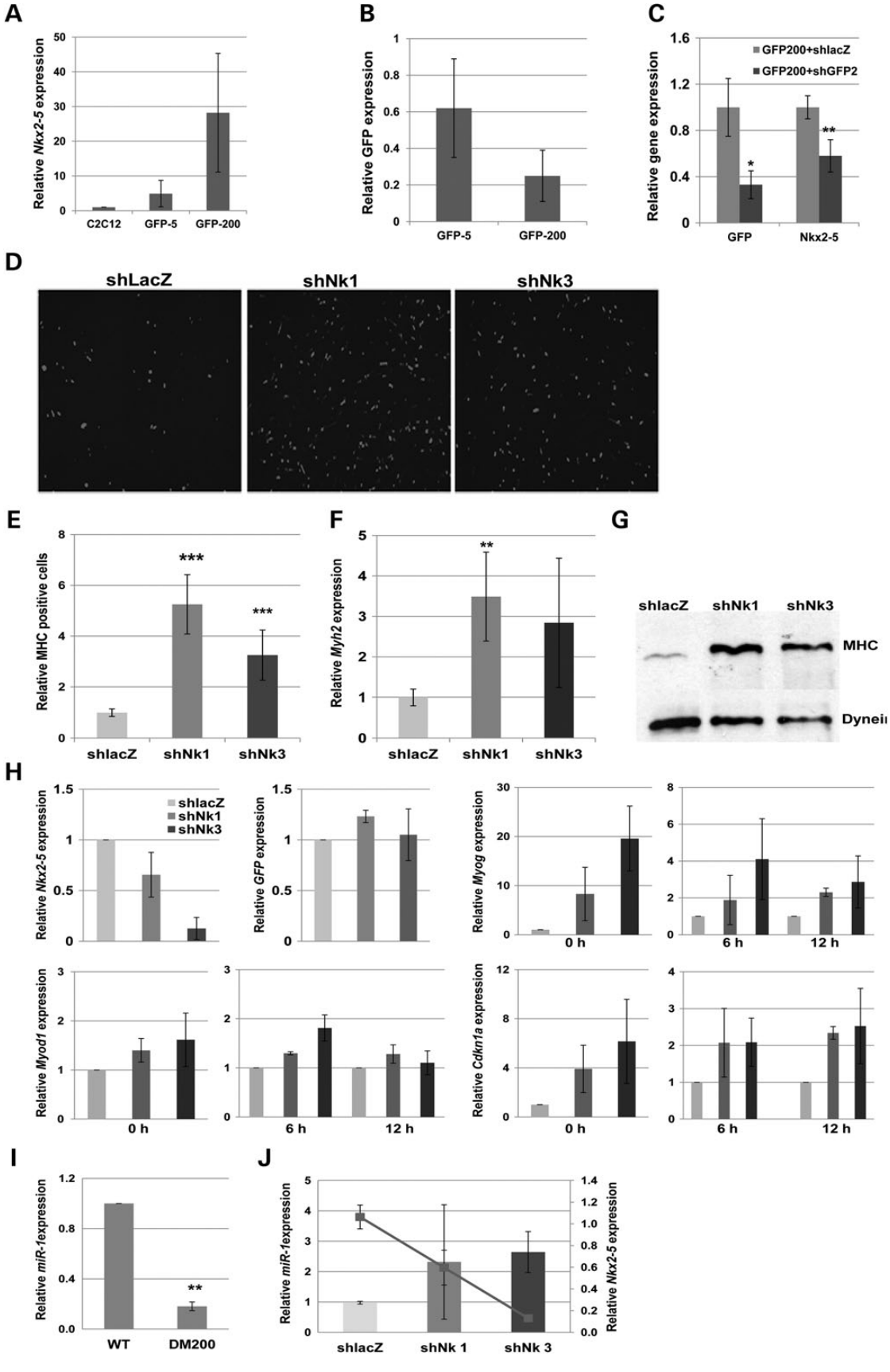
A
Relative Nkx2-5 expression
C2C12
GFP-5
GFP-200
B
Relative GFP expression
GFP-5
GFP-200
C
GFP200+shlacZ
GFP200+shGFP2
Relative gene expression
GFP
Nkx2-5
D
shLacZ
shNk1
shNk3
E
Relative MHC positive cells
shlacZ
shNk1
shNk3
F
Relative Myh2 expression
shlacZ
shNk1
shNk3
G
shlacZ
shNk1
shNk3
MHC
Dynein
H
shlacZ
shNk1
shNk3
Relative Nkx2-5 expression
Relative GFP expression
Relative Myog expression
Relative Myod1 expression
Relative Cdkn1a expression
0 h
6 h
12 h
I
Relative miR-1expression
WT
DM200
J
Relative miR-1expression
Relative Nkx2-5 expression
shlacZ
shNk 1
shNk 3

with the GFP-5 cells (Fig. 2B), demonstrating that both repeat length and overall quantity of *DMPK* 3′UTR mRNA are capable of increasing *Nkx2-5* expression.

To confirm that the increased *Nkx2-5* expression in the GFP-200 cells was due to this mRNA, we used short hairpin RNAs (shRNAs) against GFP to knockdown toxic RNA expression. Using qRT-PCR for GFP mRNA, we consistently found ($n = 6$ independent transfections) that the shRNA reduced GFP expression by about 70% as compared with control experiments using a non-specific shRNA ($P < 0.014$). Concomitantly, we found an approximately 30% reduction in *Nkx2-5* mRNA as compared with controls ($P < 0.004$), demonstrating that induction of *Nkx2-5* expression is directly related to the expression of mutant *DMPK* 3′UTR transcripts (Fig. 2C).

We have previously shown that myogenic differentiation defects in the C2C12 RNA toxicity model are associated with reduced levels of MyoD, p21 and myogenin (5,6). To determine whether over-expression of NKX2-5 also plays a role in the myogenic defects, we transiently transfected the GFP-200 cells with plasmids expressing shRNA sequences against *Nkx2-5*. This enabled reduction of *Nkx2-5* expression in cells that continued to express the toxic RNA. Subsequently, the cells were differentiated for 3 days and then analyzed for myosin heavy chain (MHC) expression by immunofluorescence, western blotting and qRT-PCR. As shown in Figure 2D and E, immunostaining for MHC expression revealed a clear increase in its expression in cells treated with *Nkx2-5* shRNA as compared with control shRNA ($P < 0.001$ for shNk1 and shNk3). This was also confirmed by qRT-PCR ($P = 0.005$ for shNk1 and $P = 0.06$ for shNk3) and western blot analysis for MHC (Fig. 1F and G). We confirmed that the different *Nkx2-5* shRNAs caused a 50–90% reduction in *Nkx2-5* mRNA ($P = 0.25$ for shNk1 and $P = 0.0005$ for shNk3) while leaving the toxic RNA expression (GFP) unaffected (Fig. 2H). These results show that key aspects of the myogenic defects associated with the toxic RNA are mediated through induced *Nkx2-5* over-expression.

To determine which steps in myogenic differentiation are affected by Nkx2-5, we also analyzed the expression of *Myod1*, *Myog* and *Cdkn1a* (p21) mRNAs by qRT-PCR in cycling and differentiating cells (6 and 12 h after induction of differentiation) treated with the *Nkx2-5* shRNAs (Fig. 2H). The expression of *Myod1* was not affected by reduced levels of *Nkx2-5* expression. However, *Myog* mRNA increased up to 20-fold in cycling cells, and 2- to 4-fold in differentiating cells. We also found *Cdkn1a* mRNA is increased in cycling cells up to 6-fold and 2-fold in differentiating cells. We also looked at miR-1 in cycling DM200 cells. miR-1 is another factor important for proper myogenic differentiation and has been previously shown to be regulated by NKX2-5(27). We found an 80% reduction of miR-1 in the DM200 cells ($P < 0.01$) (Fig. 2I). In DM200 cells treated with the *Nkx2-5* shRNAs, we found that as *Nkx2-5* levels fell there was a corresponding increase in miR-1 levels ($P = 0.05$ for miR-1 levels using shNk3) (Fig. 2J). These results demonstrate that in cells expressing the toxic RNA, increased *Nkx2-5* contributes to the down-regulation of *Myog*, *Cdkn1a* and miR-1, factors essential to the proper regulation of myogenic differentiation.

Over-expression of NKX2-5 inhibits C2C12 myogenic differentiation

To directly study the effects of NKX2-5 on myogenic differentiation, we made C2C12 cell lines over-expressing *Nkx2-5*. Upon differentiation, these cells failed to fuse and form myotubes (Fig. 3A). In these cells, *Nkx2-5* mRNA was increased 15-fold in growth conditions (d0), and 8-fold in differentiating conditions (48 h, d2) as compared with wild-type C2C12 cells (Fig. 3B). We also analyzed the expression of *Myod1*, *Myog* and *Cdkn1a* in growth and differentiation promoting conditions by qRT-PCR and western blotting (Fig. 3B and C). We found that mRNA expression of *Myog*, but not *Myod1*, is reduced in conditions of growth (by 90%) as well as differentiation (by 75%) in cells over-expressing NKX2-5. These results were supported by western blotting. Additionally, we found that p21 protein levels were dramatically reduced under differentiation conditions, despite only a modest (20–30%) decrease in the *Cdkn1a* mRNA. Analysis by qRT-PCR also showed a >50% reduction in *Myh2* mRNA expression in cells differentiated for 2 and 4 days (Fig. 3B). Consistent with this, we found reduced levels of MHC expression by western blotting (Fig. 3C).

When miR-1 was measured by qRT-PCR in these cell lines, we found a statistically significant decrease in miR-1 levels ($P = 0.04$) (Fig. 3D). It has been demonstrated that over-expression of NKX2-5 in HL-1 cells (a mouse cardiomyocyte cell line) led to a reduction in miR-1, while *Nkx2-5*$^{-/-}$ mouse embryos had an increase in miR-1 levels relative to controls (27). Furthermore, this group identified a 2.6-kb miR-1 enhancer region containing four NKX2-5 binding sites, that when mutated, rendered transcription from a luciferase reporter gene insensitive to NKX2-5 levels, demonstrating that NKX2-5 acted as a transcriptional repressor of miR-1 expression. To confirm these findings in our C2C12 cell lines, we generated a luciferase construct containing the four NKX2-5 sites. When transfected into our NKX2-5 over-expression cell line, we also

Figure 2. Increased NKX2-5 in a C2C12 model of RNA toxicity contributes to myogenic differentiation defects. (**A**) qRT-PCR of *Nkx2-5* mRNA in cells expressing GFP-*DMPK* 3′UTR $(CTG)_5$ and $(CTG)_{200}$. (**B**) qRT-PCR of GFP expression in cells expressing GFP-*DMPK* 3′UTR $(CTG)_5$ and $(CTG)_{200}$. (**C**) qRT-PCR of GFP-*DMPK* 3′UTR $(CTG)_{200}$ mRNA and *Nkx2-5* mRNA after transfection of cells with either shRNA against GFP (shGFP2) or a control shRNA (shLacZ) shows *Nkx2-5* expression is responsive to the level of toxic RNA. GFP and *Nkx2-5* mRNA were normalized to *Gapdh* mRNA. (**D**) Immunofluorescence of MHC in GFP-200 cells at 3 days post-differentiation shows that cells transfected with *Nkx2-5* shRNA (shNk1, shNk3) have increased MHC staining as compared with control (shLacZ). (**E**) Quantification of MHC positive cells relative to the total number of nuclei per visual field in cells treated with *Nkx2-5* shRNA; *P* values as indicated ($n = 4$ independent transfections/shRNA). (**F**) qRT-PCR of *Myh2* expression after transfection with indicated shRNA constructs ($n = 4$ independent transfections/shRNA). (**G**) Western blot of MHC in GFP-200 cells transfected with different *Nkx2-5* shRNAs (shNk1, shNk3) shows increased MHC; shLacZ-transfection control; dynein-loading control. (**H**) qRT-PCR shows that shNk1 and shNk3 significantly reduce *Nkx2-5* mRNA levels without major effects on *GFP* or *MyoD* mRNAs in GFP-200 cells, while rescuing *Myog*, and *Cdkn1a* mRNA expression. All results were normalized to *Gapdh* mRNA, and to results from cells treated with (shLacZ), a negative control. (**I**) qRT-PCR in the GFP-200 cells shows significantly decreased miR-1expression. (**J**) qRT-PCR of miR-1 expression (shaded bars and left axis scale) and *Nkx2-5* expression (gray line and right axis scale) after transfection with indicated shRNA constructs ($n = 4$ independent transfections/shRNA). Statistical significance $^{*}P < 0.05$, $^{**}P < 0.01$, $^{***}P < 0.001$; $n \geq 3$ for all experiments; error bars are $\pm$SD.

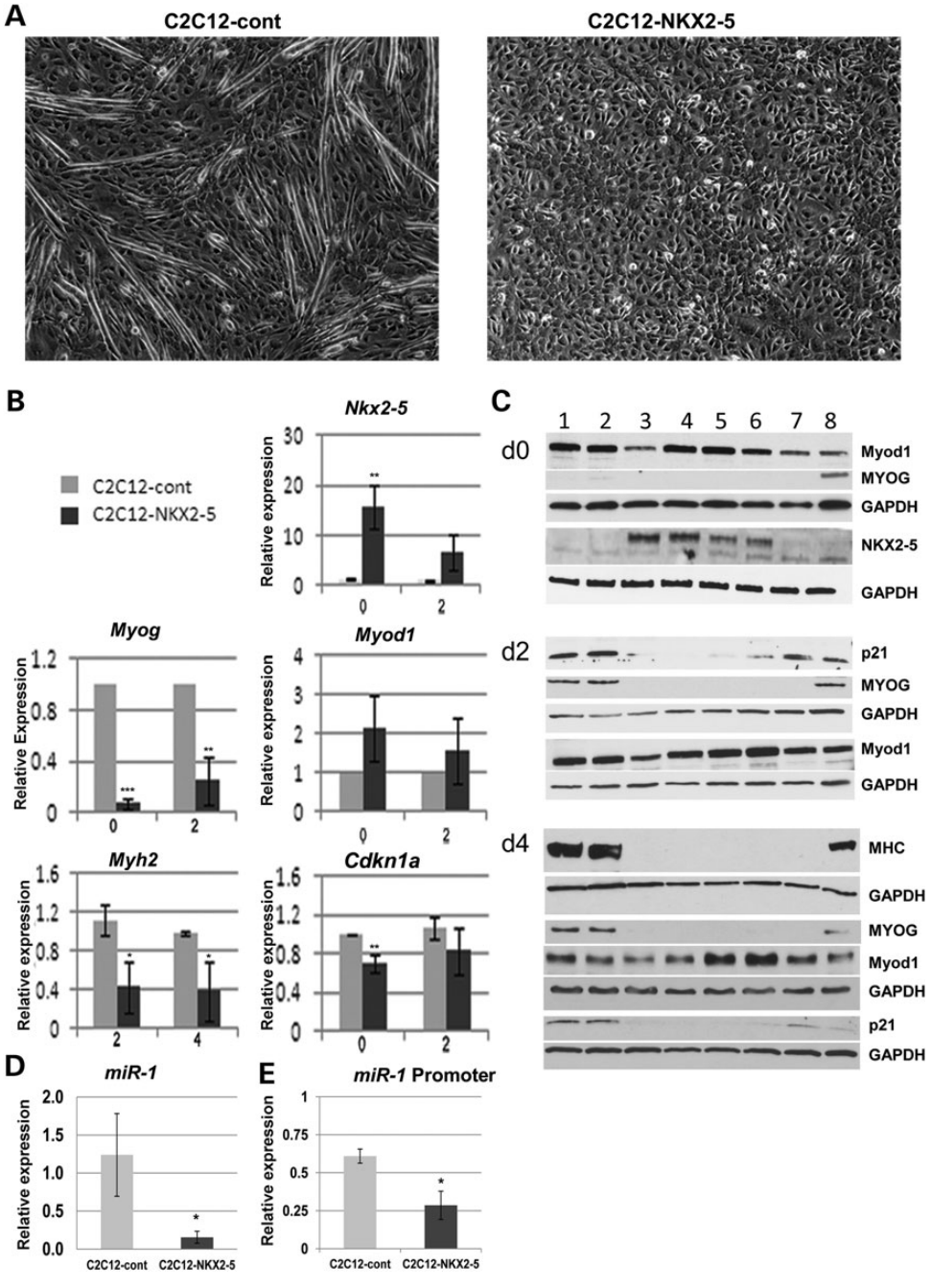

Figure 3. NKX2-5 over-expression inhibits C2C12 myogenic differentiation. (**A**) Phase contrast microscopy ($\times 100$) shows lack of myotubes 4 days post-differentiation induction in C2C12 cells over-expressing NKX2-5 (right panel) as compared with C2C12 cells expressing the control plasmid. (**B**) qRT-PCR of *Nkx2-5*, *Myod1*, *Myog*, *Cdkn1a* and *Myh2* mRNA; all results normalized to *Gapdh* mRNA and then normalized to results from the control C2C12 cells for each time point (0, 2 and 4 days of differentiation). (**C**) Western blots show reduced levels of key myogenic differentiation markers myogenin (MYOG) and P21, and MHC in four different stable C2C12-NKX2-5 cell lines (lanes 3–6) as compared with two different C2C12-control cell lines (lanes 1–2), whereas MyoD1 is unaffected. Lane 7 is an extract from cycling wild-type C2C12 cells, and lane 8 is an extract made from C2C12 cells after 3 days in differentiation media; GAPDH-loading control; days in differentiation media are indicated (d0, d2, d4). (**D**) qRT-PCR of *miR-1* in C2C12-NKX2-5 cells as compared with C2C12-control cells. (**E**) Luciferase units relative to control from a transfected luciferase construct containing the 2.6-kb miR-1-1 enhancer with four Nkx2-5 binding sites. Statistical significance $^{*}P < 0.05$, $^{**}P < 0.01$, $^{***}P < 0.001$; $n \geq 3$ for all experiments; error bars are $\pm$ SD.

saw a decrease in luciferase levels relative to the control C2C12 lines ($P = 0.015$) (Fig. 3E).

These results demonstrate that NKX2-5 over-expression in differentiating myoblasts has striking, deleterious effects on myogenin, p21 and miR-1, all key players in the myogenic differentiation process. They are also consistent with the data shown in Figure 2, in which the knockdown of *Nkx2-5* in C2C12 cells expressing the toxic RNA achieved a substantial rescue of myogenin, p21 and miR-1 levels and myogenic differentiation.

NKX2-5 modifies phenotypic severity in a mouse model of RNA toxicity

To examine the role of NKX2-5 over-expression in skeletal muscle, we generated a NKX2-5 over-expressing transgenic mouse line (TgNkx2-5) under the control of the same *DMPK* promoter used to make the RNA toxicity mice. This promoter was chosen so that NKX2-5 tissue expression would mirror that of the toxic RNA expression. The TgNkx2-5 mice were born smaller than their wild-type littermates and had an increased mortality (Fig. 4A–C). While not limited to skeletal muscle, NKX2-5 expression was clearly detected in muscle by western blot and immunofluorescence staining (Fig. 4D and E). Levels of the protein and RNA were within the ranges observed in the severely affected DM1 samples. Using functional assays, we determined that these mice had decreased grip strength as early as 1 month of age and were less capable of running as compared with their control littermates (Supplementary Material, Fig. S5). Interestingly, their skeletal muscle showed no striking histopathology, and the fiber size distribution was similar between the TgNkx2-5 mice and the wild-type control littermates (Fig. 4F). However, *Myog* ($P = 0.05$) and miR-1 ($P = 0.13$) levels were decreased similar to the results seen in the NKX2-5 over-expressing C2C12 cell lines (Fig. 4G).

To determine if increasing levels on NKX2-5 can modify DM1 phenotypes, we crossed the TgNkx2-5 mice to homozygous DM5-313$^{+/+}$ mice. The resulting offspring (TgNkx2-5/5-313$^{+/-}$ and 5–313$^{+/-}$) were either induced with the administration of doxycycline or left uninduced as controls. After 4 weeks of induction, the mice over-expressing NKX2-5 had significant decreases in retained grip strength ($P = 0.011$) and run distance ($P = 0.001$) as compared with the induced 5–313$^{+/-}$ littermates (Fig. 5A). In addition, skeletal muscle histopathology was worse, with an increased number of small fibers compared with the control littermates (Fig. 5B and Supplementary Material, Table S1). These results showed that NKX2-5 is a modifier, as over-expression of NKX2-5 worsened the effects of RNA toxicity in our mice.

However, as we only had one line of mice over-expressing NKX2-5, we sought alternative ways to determine if NKX2-5 modifies RNA toxicity. On the basis of the above results, we inferred that reducing NKX2-5 levels may lessen the effects of RNA toxicity. To test this hypothesis, we crossed the 5–313 mice with mice that had reduced NKX2-5 levels (*Nkx2-5*$^{LacZ/+}$) (17,28). The *Nkx2-5*$^{LacZ/+}$ mouse contains a *LacZ* cassette in the first exon of the *Nkx2-5* gene. Homozygous mice from this line are embryonic lethal, but the heterozygotes are healthy and viable with no evident muscle pathology. We confirmed

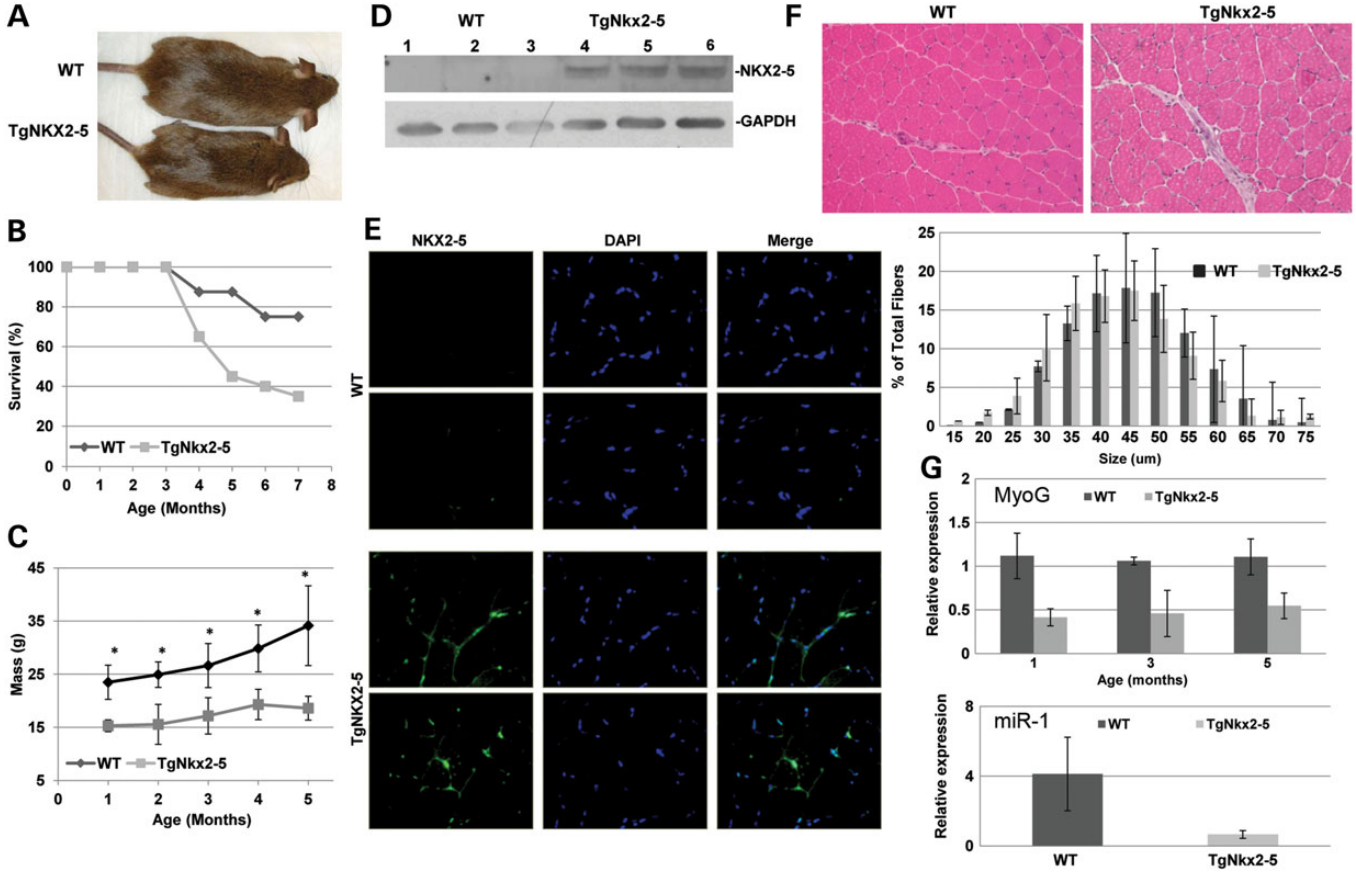

Figure 4. Characterization of TgNkx2-5 mice. (**A**) Picture of TgNkx2-5$^{+/-}$ mice as compared with wild-type littermates. (**B**) TgNkx2-5 mice ($n = 20$) have a shortened survival and (**C**) lower mass compared with wild-type littermates ($n = 8$). (**D** and **E**) Western blot and immunofluorescence showing expression of NKX2-5 in skeletal muscle. (**F**) Muscle sections from TgNkx2-5 mice ($n = 5$) and control littermates ($n = 3$) appear normal (H&E pictures) and have similar fiber size distributions (graph). (**G**) *Myogenin* ($n = 5$/group) (upper graph) and miR-1 ($n = 7$/group) (lower graph) levels are affected in the TgNkx2-5 mice compared with control littermates. Statistical significance $^{*}P < 0.05$, $^{**}P < 0.01$, $^{***}P < 0.001$; Error bars are ± SD (for 4A-F) and ± SEM (for 4G).

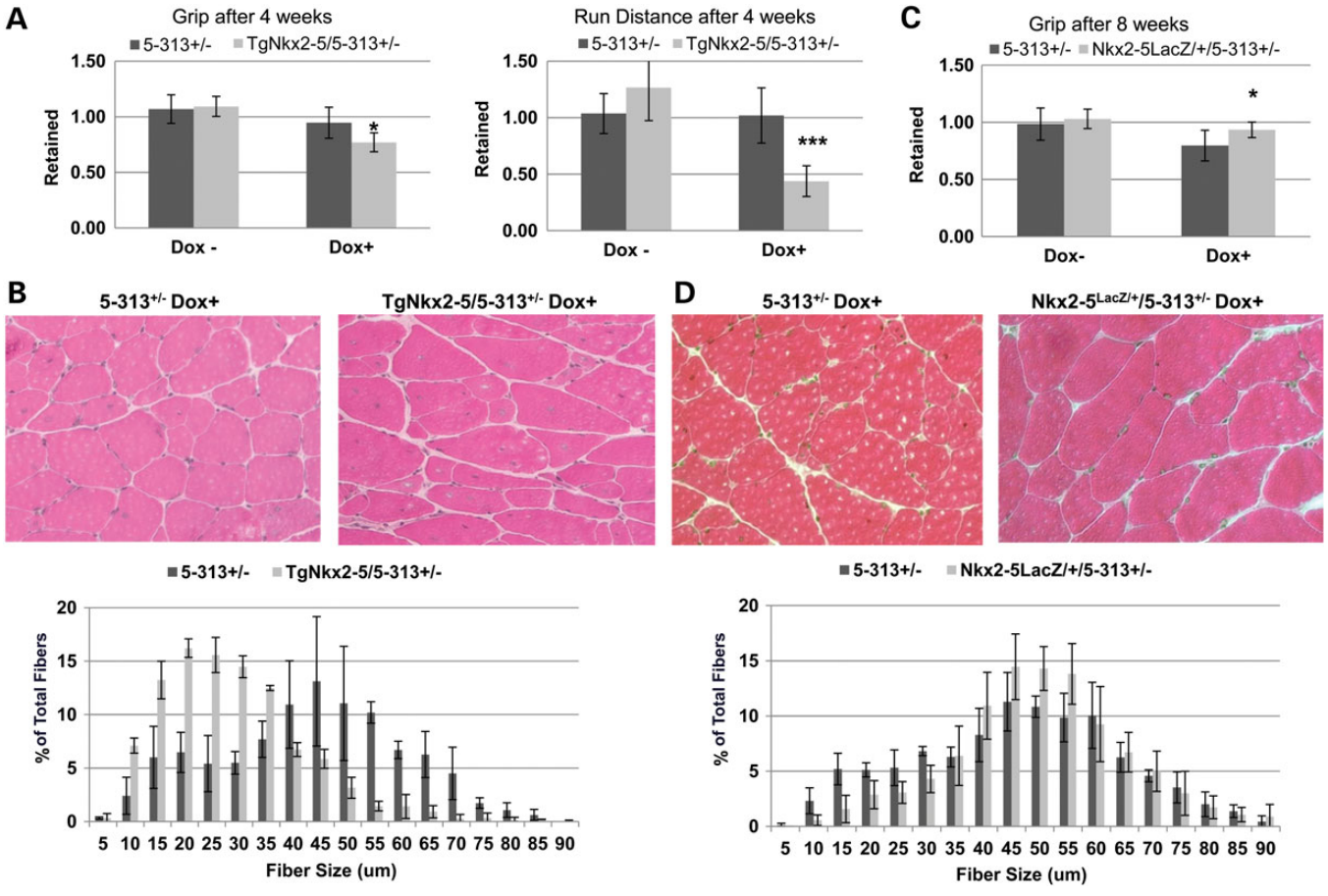

Figure 5. NKX2-5 levels modify the RNA toxicity phenotype. (**A**) Grip strength and run distance ($n = 6–9$) is decreased in induced DM5-313 mice over-expressing NKX2-5. (**B**) Histopathology is more severe in these mice (H&E), as measured by fiber size analysis (graph), as compared with the induced DM5-313 mice ($n \geq 3$/group). (**C**) In induced mice with NKX2-5 haploinsufficiency (*Nkx2-5*$^{LacZ/+}$/5-*313*$^{+/-}$), grip strength is less affected as compared with induced 5–313 mice ($n \geq 7$/group). (**D**) Histopathology in the *Nkx2-5*$^{LacZ/+}$/5-*313*$^{+/-}$ mice is less severe (H&E), as measured by fiber size analysis (graph) as compared with the induced 5-*313*$^{+/-}$ mice ($n \geq 3$/group). Error bars are $\pm$SD.

that the *Nkx2-5*$^{LacZ/+}$ mice had reduced expression of *Nkx2-5* (Supplementary Material, Fig. S6) (17). In the *Nkx2-5*$^{LacZ/+}$/5-313$^{+/-}$ mice induced for RNA toxicity, we saw a trend towards better grip strength as early as 2 and 4 weeks after induction and significant improvement in the muscle grip strength by 8 weeks of induction ($P = 0.015$) as compared with the 5–313$^{+/-}$ induced littermates (Fig. 5C). Additionally we observed an improvement in muscle histopathology as measured by fiber diameter (Fig. 5D and Supplementary Material, Table S2). Notably, the reduction in Nkx2-5 did not alter *Mbnl1* mRNA levels as assessed by qRT-PCR, nor change the RNA splicing changes defects present in the 5–313$^{+/-}$ mice (Supplementary Material, Fig. S7). We also used another Nkx2-5 deficient transgenic mouse line, *Nkx2-5*$^{Cre/+}$, in which an IRES/Cre cassette was inserted into the 3′UTR of the *Nkx2-5* gene (29). This is thought to have generated a hypomorphic allele where NKX2-5 levels are only slightly reduced. Using these mice, we saw a trend towards increased grip strength as in the experiments with the *Nkx2-5*$^{LacZ/+}$ mice and reduced fiber size variability (Supplementary Material, Fig. S8). Taken together, these data provide strong evidence that NKX2-5 acts as a modifier of skeletal muscle pathology due to RNA toxicity.

Mice over-expressing the toxic RNA or NKX2-5 have defective muscle regeneration

The previous results clearly show that NKX2-5 is a modifier of the RNA toxicity with increased NKX2-5 leading to a worsened skeletal muscle histopathology and a worsened DM1 phenotype in our mouse model, and having a strong association with increased muscle pathology in individuals with DM1. To understand how NKX2-5 levels are modifying the pathology, we considered the observed phenotypes in our animal and cell culture models. There are a number of reports showing that incorrect regulation of the myogenic targets that we have demonstrated to be affected by NKX2-5 (i.e. miR-1, p21 and myogenin), lead to defects in myogenic differentiation (5,30–32). We hypothesized that the defects observed in the cell culture models could translate into skeletal muscle regeneration defects in mice.

To examine the effects of RNA toxicity on regeneration, we utilized a widely used injury-induced muscle regeneration model (33–35). The injection of cardiotoxin (CTX) into muscle induces inflammation and myofiber degeneration that is followed by muscle regeneration. We used DM5-313$^{+/-}$

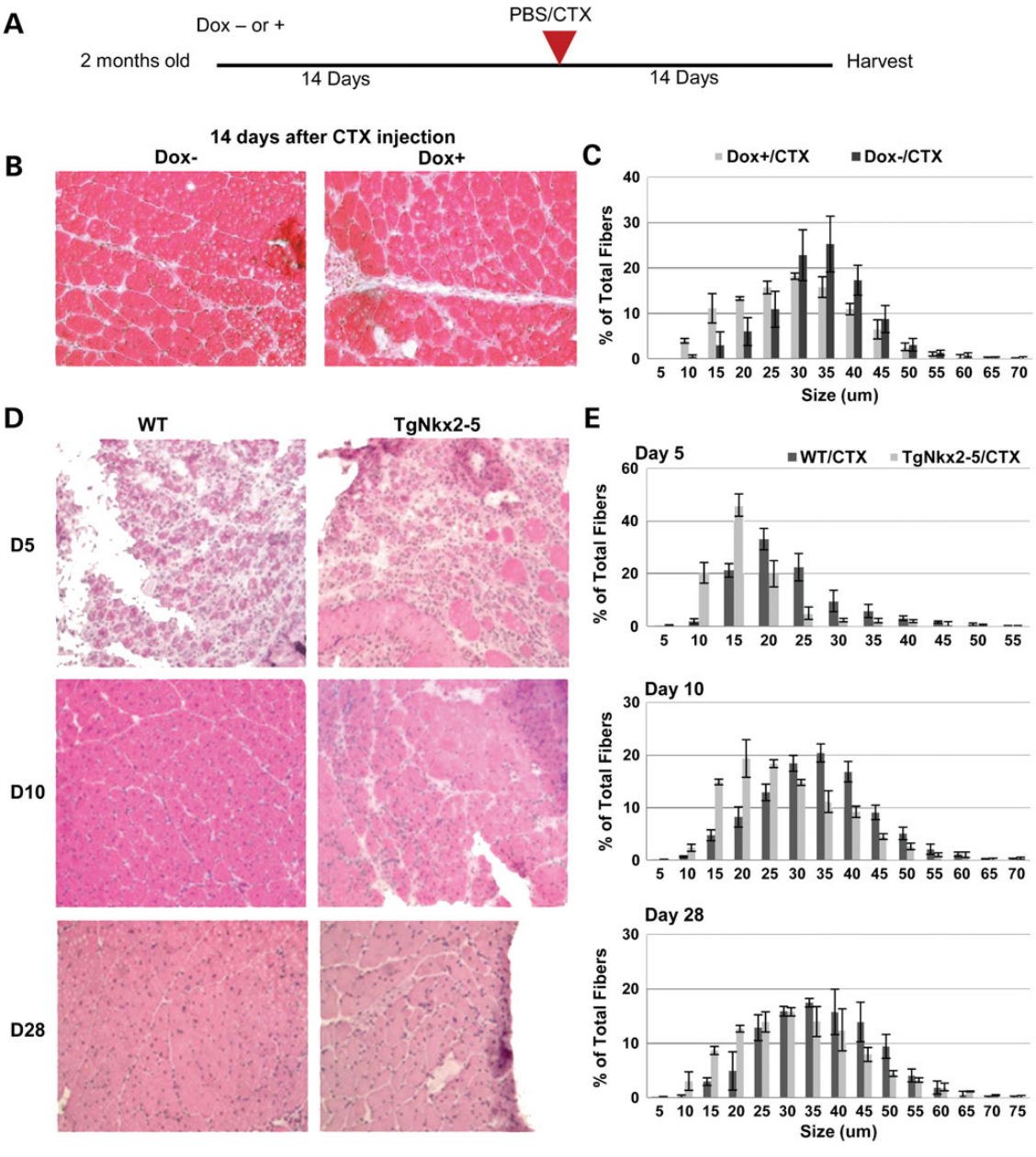

Figure 6. Muscle regeneration defects are present in mice with RNA toxicity or with NKX2-5 over-expression. (**A**) Schema of the CTX damage/regeneration study. (**B**) Histology of induced or uninduced DM5$^{+/-}$ mice 14 days post CTX injection. (**C**) Muscle fiber size distribution in CTX injected, induced and uninduced DM5 mice. The induced CTX injected mice had a greater percentage of smaller fibers. (**D** and **E**) Histology and analysis of fiber size distribution 5, 10 and 28 days after either phosphate buffered saline (PBS) or CTX injection in TgNkx2-5 mice show an increase in smaller fibers in the NKX2-5 over-expressing mice. Data represented as mean $\pm$ SD; $n = 3$/group.

mice, which upon induction of RNA toxicity develop DM1 histopathology slowly. DM5-313$^{+/-}$ mice were either uninduced or induced for 14 days. At this point, the gastrocnemius muscles in each mouse were injected with either CTX or phosphate buffered saline (PBS) (in the contralateral leg) (Fig. 6A). Tissues were collected at various days post-injection for further analyses. A more severe histopathology and significant differences in fiber size distributions were observed when comparing the induced and uninduced groups that received the CTX injection ($P < 0.03$) (Fig. 6B, C and Supplementary Material, Table S3). The induced group had both a smaller median fiber size in the damaged sections and an increase in the number of small fibers (fiber diameter $\leq$15–20 μm). Additionally, the CTX damaged, DM5-Dox+ mice had a greater number of central nuclei still present in the damaged section. Notably, in the PBS-injected muscle of the uninduced and induced mice, the fiber size distribution and morphology were similar at 14-day post-injection (Supplementary Material, Table S3), showing that 4 weeks of RNA toxicity did not significantly alter the histopathology of the muscles. All of these observations are consistent with a delayed regenerative process and demonstrate that regeneration defects are present in the skeletal

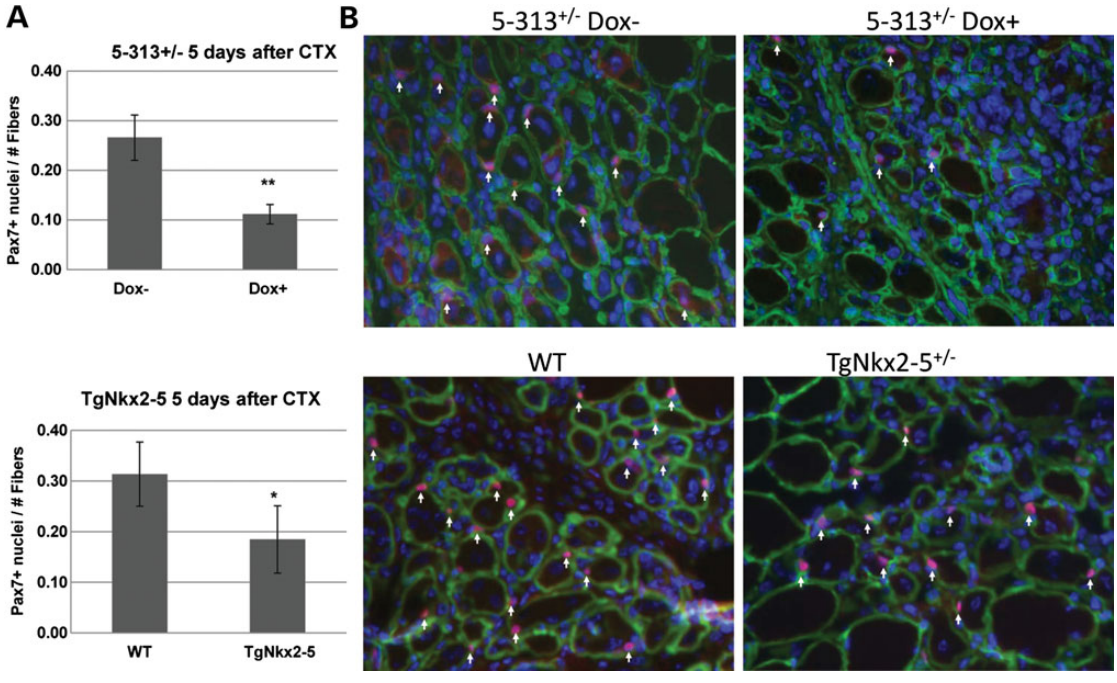

Figure 7. Satellite cell number is decreased by RNA toxicity or NKX2-5 over-expression. (**A**) Quantification of Pax7 positive nuclei per myofiber in 5-313$^{+/-}$ mice 5 days after CTX damage shows RNA toxicity (Dox+) reduced PAX7 + nuclei. (**B**) Quantification of Pax7 positive nuclei per myofiber in TgNkx2-5 mice 5 days after CTX damage shows reduced PAX7+ve nuclei as compared with wild-type mice. Representative PAX7 immunofluorescence images are presented (arrowheads indicate PAX7+ve nuclei). Pax7—red; laminin—green; nuclei—blue. Data represented as mean ± SD; $n = 3–5$ per group.

muscle of the mice with RNA toxicity even at a time point when there is no significant histopathology.

We went on to determine if the CTX injury model resulted in similar regeneration defects in the TgNkx2-5 mouse model. We found that as early as 5-day post injury and as late as 28 days, there was an increase in small fibers in the TgNkx2-5$^{+/-}$ mice as compared with the wild-type controls (Fig. 6D and E). Thus, over-expression of NKX2-5 results in regeneration defects similar to those caused by RNA toxicity.

Skeletal muscle regeneration relies upon muscle precursor cells known as satellite cells, which are normally quiescent but proliferate rapidly in response to damage and subsequently differentiate into myoblasts that fuse and regenerate muscle fibers. The transcription factor PAX7 plays a key role in satellite cells and is used commonly as a marker of satellite cells. Using PAX7 immunofluorescence as a marker of satellite cells (and satellite cells recently committed to the myoblast lineage), we examined PAX7 expression in the skeletal muscles of our DM5-313 RNA toxicity model. In non-damaged muscle, there were approximately three PAX7+ve nuclei per 100 muscle fibers in both the DM5-313-Dox-ve and DM5-313-Dox+ve mice. The number of PAX7+ve nuclei rose to 27 per 100 fibers in skeletal muscle of uninduced DM5-313 mice 5 days after CTX damage of the muscle, at a time when satellite cell and recently committed myoblast number is at its peak (34), indicating a robust proliferative response. In contrast, under the same conditions of CTX damage in the DM5-313 Dox+mice, the number of PAX7+ve nuclei was only 11 per 100 fibers, representing a 59% reduction ($P < 0.001$) (Fig. 7A). These data clearly indicated that RNA toxicity led to a defect in satellite cell response to damage.

To evaluate if the defective regenerative response in the TgNkx2-5 mice could be due to a similar effect on satellite cells, we evaluated PAX7 expression in these mice. In non-damaged muscle, the number of PAX7+ve nuclei was roughly two per 100 muscle fibers in both the wild-type and TgNkx2-5 mice. Five days after CTX damage of the muscle, this rose to ~31 per 100 fibers in wild-type mice. However, it was only 18 per 100 fibers in the damaged tissues from TgNkx2-5$^{+/-}$ mice, representing a 41% reduction ($P = 0.014$) in the number of Pax7+ve nuclei (Fig. 7B). Thus, both RNA toxicity and NKX2-5 over-expression were both associated with a similar defect in satellite cell behavior.

DISCUSSION

Previously, we reported that RNA toxicity induced NXK2-5 expression in cardiac and skeletal muscles in our RNA toxicity mouse models and in DM1 patient tissues (17). The finding of NKX2-5 expression in skeletal muscle was unexpected. In this study, we find that in both mouse models of RNA toxicity and skeletal muscles from DM1 patients, the expression of NKX2-5 is correlated with severity of muscle histopathology (Fig. 1). Although there is some evidence that it is expressed in a limited set of skeletal muscles during embryonic development, NKX2-5 is a cardiac transcription factor that is absent in mature skeletal muscle. In DM1, RNA toxicity leads to a more embryonic pattern of gene expression and RNA splicing (36–38). The expression of NKX2-5 could be a further manifestation of this effect, but its significance is unknown. In this study, we set out to determine whether increased NKX2-5 levels have a role

in skeletal muscle pathology due to RNA toxicity associated with DM1 phenotypes.

DM1 muscle pathology is characterized by a progressive wasting of muscle that eventually leads to fibrosis and fatty infiltration. Unlike other muscular dystrophies such as DMD, where there is initially an active regeneration in skeletal muscle in response to the incurred damage, typical reports of DM1 muscle pathology often remark about the surprising lack of regeneration (8–11). The molecular basis of regeneration defects in DM1 skeletal muscle is still largely unexplored. *In vivo*, myoblasts (activated and committed satellite cells) differentiate and fuse to form new muscle fibers during muscle formation and regeneration. Recently, satellite cell dysfunction in damaged muscle fibers has been proposed for the progressive muscle wasting in DM1 (11). The authors found an increase in the number of satellite cells without an increase in regenerating fibers. Others have reported differentiation defects using primary myoblasts from DM1 patients (8–11). Moreover, recent studies have shown impairment of muscle regeneration in muscleblind-like 3 (*Mbnl3*) knockout mice (33). This is consistent with the data from our C2C12 model of RNA toxicity, where we have extensively demonstrated adverse effects of RNA toxicity on myogenesis (7). We have now also found increased *Nkx2-5* expression in this model of RNA toxicity (Fig. 2). Notably, when *Nkx2-5* expression was knocked-down in these cells without affecting toxic RNA production, the resulting rescue of the expression of key markers of myogenic progression [i.e. increased *Myh2*, *Myog*, *Cdkn1a* (p21) and miR-1 expression] showed that *Nkx2-5* over-expression contributes significantly to the myogenic defects caused by the mutant *DMPK* 3′UTR mRNA. Here, we also found that over-expression of NKX2-5 in C2C12 myoblasts also inhibits differentiation and myoblast fusion (Fig. 3). Increased NKX2-5 inhibited the expression of myogenin and p21, key players in myogenic differentiation along with miR-1, a microRNA (miRNA) shown to be vital for myogenic differentiation (30,39). Of note, the effect on p21 may be mediated through additional miRNA regulation, as NKX2-5 has been shown also to affect the expression of the miR-17-92 cluster, which has been shown to affect p21 (40,41).

Although cell culture myoblast models, such as our C2C12 model of RNA toxicity, have a defined utility in studying aspects of RNA toxicity, there are limitations to extrapolating the results to an *in vivo* situation. Therefore, we used mouse models to study the effects of NKX2-5 and RNA toxicity. The eGFP transgene expressing the toxic RNA was driven by a human *DMPK* promoter in an attempt to mimic the expression of *DMPK* (13). To reproduce the expression pattern of the toxic RNA, we used the same promoter construct to generate NKX2-5 transgenic mice. This proved rather difficult, as repeated attempts over several years yielded only one transgenic line expressing NKX2-5 (the TgNkx2-5). This is probably a reflection of the sensitivity of the heart to varying NKX2-5 levels (42–44). It is likely that the moderate over-expression of NKX2-5 in the hearts of TgNkx2-5 mice (2- to 3-fold) enabled them to survive, albeit with a shortened lifespan (Fig. 4). Importantly, for the purposes of this study, NKX2-5 was expressed in skeletal muscle. Although over-expression of NKX2-5 did not have any overt effects on the histology of the skeletal muscle, the deleterious effects were clearly evident in the molecular effects on *Myog* and miR-1 (Fig. 4) and in functional assays such as grip strength and treadmill running (Supplementary Material, Fig. S6). Furthermore, the beneficial and detrimental effects on these phenotypes of decreasing or increasing (respectively) the amount of NKX2-5 present in our 5–313 mice (Fig. 5) demonstrate the functional relevance of NKX2-5 as a modifier of skeletal muscle phenotypes in RNA toxicity.

How does NKX2-5 do this? The consequences of modulating NKX2-5 levels in mice with RNA toxicity provided some clues. RNA toxicity in the 5–313 mice led to a more severe DM1-like histopathology and a significant skew in fiber size towards small fibers (Supplementary Material, Fig. S9 and Fig. 5). Over-expression of NKX2-5 clearly worsened this while haploinsufficiency had noticeable benefits (Fig. 5). This suggested that NKX2-5 somehow impaired the response to damage caused by the toxic RNA. The CTX experiments enabled us to study this in a more defined and well-characterized manner, revealing that TgNkx2-5 mice had a regeneration defect in response to muscle damage (Figs 6 and 7). Our results with CTX injection in the 5–313 mice show that delayed muscle regeneration is an early effect of RNA toxicity, even before the onset of detectable muscle histopathology (Fig. 6B and C). Satellite cells are the key mediators of muscle regeneration. Our analyses of the TgNkx2-5 mice and the DM5-Dox+ve mice, showing the reduced number of PAX7+ve nuclei in response to induced damage, point to defects in satellite cell function and subsequent progression to committed myoblasts capable of regeneration (Fig. 7). These potentially synergistic effects of RNA toxicity and NKX2-5 over-expression are consistent with the concept of defective regenerative capacity in DM1, where repeated cycles of damage are not met with an adequate or sufficient regenerative response, leading to progressively worsening muscle pathology.

Muscular dystrophy in DM1 is likely due to a complex set of changes in gene expression induced by the toxic RNA, including effects on RNA-binding proteins such as MBNL1-3 and CELF1, a plethora of splicing defects and other as yet defined alterations. Here, we clearly show that NKX2-5 acts as a modifier of skeletal muscle pathology induced by RNA toxicity using correlative studies in human tissues, as well as a variety of mechanistic studies using cell culture and mouse models. These results support the hypothesis that increased expression of NKX2-5 in skeletal muscle is deleterious to myogenesis and muscle regeneration and contributes to muscle wasting and weakness caused by RNA toxicity.

MATERIALS AND METHODS

Ethical statement

All studies on human subjects were done under the auspices of the University of Virginia Institutional Review Board. All studies utilizing mice were done under the auspices of the University of Virginia Animal Care and Use Committee.

Patient samples

Human tissue samples were obtained from the University of Miami Tissue Bank, Dr Charles A. Thornton (University of Rochester, USA) and Dr Laura P. Ranum (University of Minnesota, USA).

All DM1 ($n = 8$) and DM2 ($n = 2$) tissues were from patients with diagnoses confirmed by molecular analyses. Muscle samples from patients with other muscle disorders: DMD ($n = 3$), X-linked myopathy ($n = 1$) as well as four non-muscular dystrophy tissues were also studied. All studies were done under the auspices of the University of Virginia Institutional Review Board. Quantitative histopathological grading was done as outlined in the supplemental methods.

Transgenic mice

Characterization of transgenic mice are described elsewhere (13). We used two different *DMPK* 3′UTR mRNA transgenic lines (5–313 and 5–336) (FVB strain). Chloride channel 1 (SWR/J-Clcn1$^{adr\text{-}mto}$/J), MDX (C57BL/10ScSn-*Dmd*^{mdx}/J) and GFP (C57BL/6-Tg (tetO-CDK5R1/GFP) 337Lht/J) mice were obtained from The Jackson Laboratory (Bar Harbor, Maine). Tissues from HSA-LR mice (22) were provided by Dr C.A. Thornton. Tissues from the Mbnl1$^{-/-}$ and a Mbnl1$^{-/-}$/Mbnl2$^{+/-}$ mice were provided by Dr Swanson (26). The *Nkx2-5*$^{LacZ/+}$ mice (17,28) and the *Nkx2-5*$^{Cre/+}$ mice (29) were provided by Dr R.P. Harvey. The TgNkx2-5 line was generated using the 5–313 cloning vector but replacing the GFP and DMPK 3′UTR with the cDNA for mouse *Nkx2-5*. Unfortunately, the resultant mouse line was unresponsive to doxycycline but was constitutively active.

Histology

H&E staining was done using standard procedures. Fiber size was determined by measuring cross-sectional area of each muscle fiber in a ×200 image of H&E-stained skeletal muscle. Five mice per group were analyzed and for each mouse, at least three images were analyzed.

Cell culture and reagents

C2C12 myoblasts were maintained at subconfluent densities in Dulbecco's modified eagle medium (DMEM) supplemented with 10% fetal bovine serum (growth media, GM). To induce myoblast differentiation, cells were grown to 90% confluence and then cultured in differentiation media containing DMEM supplemented with 2% horse serum (HyClone®). Differentiation media was replaced every 24 h. Stable C2C12 clones expressing the GFP-*DMPK* 3′UTR with either $(CTG)_5$ or $(CTG)_{200}$ were obtained by transfection using the Nucleofector™ kit from Amaxa™ and selection for 9 days with 800 μg ml^{-1} G418 (Gibco®). Four independent clones for each construct were used for subsequent analyses. Stable C2C12 clones expressing NKX2-5 were obtained by transfection using a PCDNA3.1-HisC-*Nkx2-5* (open reading frame), and control cell lines with PCDNA3.1 (Invitrogen, Inc.). Eight clones for each construct were used for subsequent analyses. Primer sequences and methods for generating shRNA constructs used in this study are detailed in Supplementary Material, Table S6.

RNA analyses

Total RNA was extracted from tissues collected in isopentane and flash frozen in liquid nitrogen (10). Total RNA (1 μg) was used for making cDNA using QuantiTect™ Reverse Transcription Kit (Qiagen®) and then subjected to PCR using gene-specific primers. qRT-PCR was done using the BioRad iCycler™ and BioRad's kits using manufacturer's protocols and detected with SYBRGreen™ dye. miR-1 was analyzed using Invitrogen's NCode miRNA First-Strand cDNA Synthesis and qRT-PCR kit form 1 μg total RNA. Primer sequences are given in Supplementary Material, Tables S4 and S5. All reactions were performed with technical duplicates except in the case of miR-1 in which technical triplicates were used. Biological replicates were always greater than three and indicated in the text and figure legends. Data normalization was accomplished using the endogenous control (*Gapdh or U6*), and the normalized values were subjected to a $2^{-\Delta\Delta Ct}$ formula to calculate the fold change between the control and experimental groups. All splicing assays were done in at least three mice or more per group. mRNA splicing primers and conditions have been previously reported (15).

CTX and regeneration

DM5-313$^{+/-}$ mice were either kept on normal water (uninduced) or given 0.2% doxycycline (induced) for 14 days. After 14 days, the gastrocnemius muscles in each mouse was injected with either 10 μM CTX or PBS. After another 14 days, tissues were harvested, sectioned and stained. The muscle fiber size was determined by measuring the cross-sectional area of each muscle fiber in a ×200 image of H&E-stained skeletal muscle. Five mice per group were analyzed and for each mouse, at least three images were analyzed using AxioVision V4.8.2.0 (Carl Zeiss MicroImaging). PAX7 immunofluorescence was done with tissues collected 5 days after CTX injection. Flash frozen 6 μm sections were fixed with 4% paraformaldehyde. Primary antibodies were anti-Pax7 (DSHB, Pax7-c; 1:50 dilution) and anti-laminin (Sigma, #L9393; 1:200 dilution). Secondary antibodies were from Molecular Probes™ (1:1000 dilutions).

Immunoblotting and immunofluorescence

Tissues were collected in isopentane and flash frozen in liquid nitrogen. Protein extracts were made in radioimmunoprecipitation assay buffer (50 mM Tris–HCl, pH 7.4, 150 mM NaCl, 1% NP40, 0.5% Na-deoxycholate, 0.1% sodium dodecyl sulfate [SDS]) and protease inhibitor (Roche). Protein extracts from cells were made in cell lysis buffer (50 mM HEPES, pH 7.6, 150 mM NaCl, 10% glycerol, 1% Triton X-100, 1.5 mM $MgCl_2$, 0.1 mM EDTA and 0.5 mM DTT) with protease inhibitors. Extracts were separated by sodium dodecyl sulfate—polyacrylamide gel electrophoresis (SDS–PAGE) and assayed by western blotting. The following antibodies were used: NKX2-5 [Santa Cruz Biotechnology® (SCBT), 1:1000 for NKX2-5 in C2C12] followed by rabbit anti-goat (SCBT, 1:5000); MYOD1 (BD Pharmingen™, 1:2000), MY-32 (Sigma-Aldrich®, 1:2000), GAPDH (Ambion®, 1:100 000) followed by goat anti-mouse (Pierce®, 1:200 00); NKX2-5 (SCBT, 1:1000 for human samples), Myogenin (SCBT, 1: 2000) and p21

(SCBT, 1:250) followed by goat anti-rabbit (Pierce®, 1:20 000). Immunofluorescence for MHC and NKX2-5 were performed as previously described (6). Microscopy was performed using an Olympus IX 50 inverted microscope with fluorescent attachments and images were captured with a CCD camera.

Statistical analyses

Standard statistical methods were employed using Minitab 16.1.0 (Minitab, Inc.). Data sets were analyzed for outliers using the Grubb's test, and once outliers were removed, the data were analyzed for normality. If normal, two-tailed student's *t*-tests were employed to assess significance, with attention paid to equal versus unequal variance and the appropriate adjustment made. Mann–Whitney assessment was used for non-normal data. Multiple comparisons were done using a one-Way ANOVA with Tukey's multiple comparisons.

AUTHOR CONTRIBUTIONS

R.Y., J.T.G., and M.S.M. designed the experiments and wrote the paper. R.Y. generated the transgenic mouse construct, stable cell lines and performed and analyzed all cell culture experiments. J.T.G. performed the miR-1 experiments and all the mouse experiments, mRNA splicing and analyses. J.T.G. graded and analyzed the mouse and human muscle sections. R.Y. performed RT-PCR and western blots on mouse and human samples. Q.Y. and M.M. were involved in all aspects of mouse breeding, genotyping, phenotyping and processing of tissues. Y.K.K. did the analysis of Nkx2-5 expression in tissues from *Mbnl* mouse models.

SUPPLEMENTARY MATERIAL

Supplementary Material is available at HMG online.

ACKNOWLEDGEMENTS

We thank Dr Charles A. Thornton and Dr Laura P. Ranum for providing DM1 and DM2 human tissues. We thank Dr Richard Harvey for providing the *Nkx2-5*$^{LacZ/+}$ and the *Nkx2-5*$^{Cre/+}$ mice. We thank Dr M.S. Swanson for the tissues from *Mbnl1*$^{-/-}$ and *Mbnl1*$^{-/-}$/*Mbnl2*$^{+/-}$ mice and Dr C.A. Thornton for tissues from the HSA-LR mice.

Conflict of Interest statement. None declared.

FUNDING

This work was supported by the National Institutes of Health (5R01AR045992 and 1R01AR062189), the Muscular Dystrophy Association (grant # 4328) and the Stone Circle of Friends.

REFERENCES

1. Mahadevan, M., Tsilfidis, C., Sabourin, L., Shutler, G., Amemiya, C., Jansen, G., Neville, C., Narang, M., Barcelo, J., O'Hoy, K. *et al.* (1992) Myotonic dystrophy mutation: an unstable CTG repeat in the 3′ untranslated region of the gene. *Science*, **255**, 1253–1255.
2. Davis, B.M., McCurrach, M.E., Taneja, K.L., Singer, R.H. and Housman, D.E. (1997) Expansion of a CUG trinucleotide repeat in the 3′ untranslated region of myotonic dystrophy protein kinase transcripts results in nuclear retention of transcripts. *Proc. Natl. Acad. Sci. USA*, **94**, 7388–7393.
3. Ranum, L.P. and Cooper, T.A. (2006) RNA-mediated neuromuscular disorders. *Annu. Rev. Neurosci.*, **29**, 259–277.
4. Amack, J.D., Paguio, A.P. and Mahadevan, M.S. (1999) Cis and trans effects of the myotonic dystrophy (DM) mutation in a cell culture model. *Hum. Mol. Genet.*, **8**, 1975–1984.
5. Amack, J.D. and Mahadevan, M.S. (2001) The myotonic dystrophy expanded CUG repeat tract is necessary but not sufficient to disrupt C2C12 myoblast differentiation. *Hum. Mol. Genet.*, **10**, 1879–1887.
6. Amack, J.D., Reagan, S.R. and Mahadevan, M.S. (2002) Mutant DMPK 3′-UTR transcripts disrupt C2C12 myogenic differentiation by compromising MyoD. *J. Cell. Biol.*, **159**, 419–429.
7. Amack, J.D. and Mahadevan, M.S. (2004) Myogenic defects in myotonic dystrophy. *Dev. Biol.*, **265**, 294–301.
8. Morgan, J.E. and Zammit, P.S. (2010) Direct effects of the pathogenic mutation on satellite cell function in muscular dystrophy. *Exp. Cell Res.*, **316**, 3100–3108.
9. Furling, D., Lemieux, D., Taneja, K. and Puymirat, J. (2001) Decreased levels of myotonic dystrophy protein kinase (DMPK) and delayed differentiation in human myotonic dystrophy myoblasts. *Neuromuscul. Disord. NMD*, **11**, 728–735.
10. Furling, D., Coiffier, L., Mouly, V., Barbet, J.P., St Guily, J.L., Taneja, K., Gourdon, G., Junien, C. and Butler-Browne, G.S. (2001) Defective satellite cells in congenital myotonic dystrophy. *Hum. Mol. Genet.*, **10**, 2079–2087.
11. Thornell, L.E., Lindstom, M., Renault, V., Klein, A., Mouly, V., Ansved, T., Butler-Browne, G. and Furling, D. (2009) Satellite cell dysfunction contributes to the progressive muscle atrophy in myotonic dystrophy type 1. *Neuropathol. Appl. Neurobiol.*, **35**, 603–613.
12. Loro, E., Rinaldi, F., Malena, A., Masiero, E., Novelli, G., Angelini, C., Romeo, V., Sandri, M., Botta, A. and Vergani, L. (2010) Normal myogenesis and increased apoptosis in myotonic dystrophy type-1 muscle cells. *Cell Death Differ.*, **17**, 1315–1324.
13. Mahadevan, M.S., Yadava, R.S., Yu, Q., Balijepalli, S., Frenzel-McCardell, C.D., Bourne, T.D. and Phillips, L.H. (2006) Reversible model of RNA toxicity and cardiac conduction defects in myotonic dystrophy. *Nat. Genet.*, **38**, 1066–1070.
14. Kim, Y.K., Mandal, M., Yadava, R.S., Paillard, L. and Mahadevan, M.S. (2014) Evaluating the effects of CELF1 deficiency in a mouse model of RNA toxicity. *Hum. Mol. Genet.*, **23**, 293–302.
15. Gladman, J.T., Mandal, M., Srinivasan, V. and Mahadevan, M.S. (2013) Age of onset of RNA toxicity influences phenotypic severity: evidence from an inducible mouse model of myotonic dystrophy (DM1). *PLoS One*, **8**, e72907.
16. Kanadia, R.N., Shin, J., Yuan, Y., Beattie, S.G., Wheeler, T.M., Thornton, C.A. and Swanson, M.S. (2006) Reversal of RNA missplicing and myotonia after muscleblind overexpression in a mouse poly(CUG) model for myotonic dystrophy. *Proc. Natl. Acad. Sci. USA*, **103**, 11748–11753.
17. Yadava, R.S., Frenzel-McCardell, C.D., Yu, Q., Srinivasan, V., Tucker, A.L., Puymirat, J., Thornton, C.A., Prall, O.W., Harvey, R.P. and Mahadevan, M.S. (2008) RNA toxicity in myotonic muscular dystrophy induces NKX2-5 expression. *Nat. Genet.*, **40**, 61–68.
18. Lints, T.J., Parsons, L.M., Hartley, L., Lyons, I. and Harvey, R.P. (1993) Nkx-2.5: a novel murine homeobox gene expressed in early heart progenitor cells and their myogenic descendants. *Development*, **119**, 419–431.
19. Komuro, I. and Izumo, S. (1993) Csx: a murine homeobox-containing gene specifically expressed in the developing heart. *Proc. Natl. Acad. Sci. USA*, **90**, 8145–8149.
20. Kasahara, H., Bartunkova, S., Schinke, M., Tanaka, M. and Izumo, S. (1998) Cardiac and extracardiac expression of Csx/Nkx2.5 homeodomain protein. *Circ. Res.*, **82**, 936–946.
21. Lyons, I., Parsons, L.M., Hartley, L., Li, R., Andrews, J.E., Robb, L. and Harvey, R.P. (1995) Myogenic and morphogenetic defects in the heart tubes of murine embryos lacking the homeo box gene Nkx2-5. *Genes Dev.*, **9**, 1654–1666.
22. Mankodi, A., Logigian, E., Callahan, L., McClain, C., White, R., Henderson, D., Krym, M. and Thornton, C.A. (2000) Myotonic dystrophy in transgenic mice expressing an expanded CUG repeat. *Science (New York, N.Y.)*, **289**, 1769–1773.
23. Mehrke, G., Brinkmeier, H. and Jockusch, H. (1988) The myotonic mouse mutant ADR: electrophysiology of the muscle fiber. *Muscle Nerve*, **11**, 440–446.

24. Bulfield, G., Siller, W.G., Wight, P.A. and Moore, K.J. (1984) X chromosome-linked muscular dystrophy (mdx) in the mouse. *Proc. Natl. Acad. Sci. USA*, **81**, 1189–1192.
25. Cruz, J.C., Tseng, H.C., Goldman, J.A., Shih, H. and Tsai, L.H. (2003) Aberrant Cdk5 activation by p25 triggers pathological events leading to neurodegeneration and neurofibrillary tangles. *Neuron*, **40**, 471–483.
26. Lee, K.Y., Li, M., Manchanda, M., Batra, R., Charizanis, K., Mohan, A., Warren, S.A., Chamberlain, C.M., Finn, D., Hong, H. *et al.* (2013) Compound loss of muscleblind-like function in myotonic dystrophy. *EMBO Mol. Med.*, **5**, 1887–1900.
27. Qian, L., Wythe, J.D., Liu, J., Cartry, J., Vogler, G., Mohapatra, B., Otway, R.T., Huang, Y., King, I.N., Maillet, M. *et al.* (2011) Tinman/Nkx2-5 acts via miR-1 and upstream of Cdc42 to regulate heart function across species. *J. Cell Biol.*, **193**, 1181–1196.
28. Biben, C., Weber, R., Kesteven, S., Stanley, E., McDonald, L., Elliott, D.A., Barnett, L., Koentgen, F., Robb, L., Feneley, M. *et al.* (2000) Cardiac septal and valvular dysmorphogenesis in mice heterozygous for mutations in the homeobox gene Nkx2-5. *Circ. Res.*, **87**, 888–895.
29. Stanley, E.G., Biben, C., Elefanty, A., Barnett, L., Koentgen, F., Robb, L. and Harvey, R.P. (2002) Efficient Cre-mediated deletion in cardiac progenitor cells conferred by a 3′UTR-ires-Cre allele of the homeobox gene Nkx2-5. *Int. J. Dev. Biol.*, **46**, 431–439.
30. Chen, J.F., Mandel, E.M., Thomson, J.M., Wu, Q., Callis, T.E., Hammond, S.M., Conlon, F.L. and Wang, D.Z. (2006) The role of microRNA-1 and microRNA-133 in skeletal muscle proliferation and differentiation. *Nat. Genet.*, **38**, 228–233.
31. Chen, J.F., Tao, Y., Li, J., Deng, Z., Yan, Z., Xiao, X. and Wang, D.Z. (2010) microRNA-1 and microRNA-206 regulate skeletal muscle satellite cell proliferation and differentiation by repressing Pax7. *J. Cell Biol.*, **190**, 867–879.
32. Rau, F., Freyermuth, F., Fugier, C., Villemin, J.P., Fischer, M.C., Jost, B., Dembele, D., Gourdon, G., Nicole, A., Duboc, D. *et al.* (2011) Misregulation of miR-1 processing is associated with heart defects in myotonic dystrophy. *Nat. Struct. Mol. Biol.*, **18**, 840–845.
33. Poulos, M.G., Batra, R., Li, M., Yuan, Y., Zhang, C., Darnell, R.B. and Swanson, M.S. (2013) Progressive impairment of muscle regeneration in muscleblind-like 3 isoform knockout mice. *Hum. Mol. Genet.*, **22**, 3547–3558.
34. Bentzinger, C.F., Wang, Y.X., Dumont, N.A. and Rudnicki, M.A. (2013) Cellular dynamics in the muscle satellite cell niche. *EMBO Rep.*, **14**, 1062–1072.
35. Orengo, J.P., Ward, A.J. and Cooper, T.A. (2011) Alternative splicing dysregulation secondary to skeletal muscle regeneration. *Ann. Neurol.*, **69**, 681–690.
36. Kalsotra, A., Xiao, X., Ward, A.J., Castle, J.C., Johnson, J.M., Burge, C.B. and Cooper, T.A. (2008) A postnatal switch of CELF and MBNL proteins reprograms alternative splicing in the developing heart. *Proc. Natl. Acad. Sci. USA*, **105**, 20333–20338.
37. Lin, X., Miller, J.W., Mankodi, A., Kanadia, R.N., Yuan, Y., Moxley, R.T., Swanson, M.S. and Thornton, C.A. (2006) Failure of MBNL1-dependent post-natal splicing transitions in myotonic dystrophy. *Hum. Mol. Genet.*, **15**, 2087–2097.
38. Du, H., Cline, M.S., Osborne, R.J., Tuttle, D.L., Clark, T.A., Donohue, J.P., Hall, M.P., Shiue, L., Swanson, M.S., Thornton, C.A. *et al.* (2010) Aberrant alternative splicing and extracellular matrix gene expression in mouse models of myotonic dystrophy. *Nat. Struct. Mol. Biol.*, **17**, 187–193.
39. Chen, J., Huang, Z.P., Seok, H.Y., Ding, J., Kataoka, M., Zhang, Z., Hu, X., Wang, G., Lin, Z., Wang, S. *et al.* (2013) mir-17-92 cluster is required for and sufficient to induce cardiomyocyte proliferation in postnatal and adult hearts. *Cir. Res.*, **112**, 1557–1566.
40. Nagel, S., Venturini, L., Przybylski, G.K., Grabarczyk, P., Schmidt, C.A., Meyer, C., Drexler, H.G., Macleod, R.A. and Scherr, M. (2009) Activation of miR-17-92 by NK-like homeodomain proteins suppresses apoptosis via reduction of E2F1 in T-cell acute lymphoblastic leukemia. *Leuk. Lymphoma*, **50**, 101–108.
41. Hong, L., Lai, M., Chen, M., Xie, C., Liao, R., Kang, Y.J., Xiao, C., Hu, W.Y., Han, J. and Sun, P. (2010) The miR-17-92 cluster of microRNAs confers tumorigenicity by inhibiting oncogene-induced senescence. *Cancer Res.*, **70**, 8547–8557.
42. Kasahara, H., Wakimoto, H., Liu, M., Maguire, C.T., Converso, K.L., Shioi, T., Huang, W.Y., Manning, W.J., Paul, D., Lawitts, J. *et al.* (2001) Progressive atrioventricular conduction defects and heart failure in mice expressing a mutant Csx/Nkx2.5 homeoprotein. *J. Clin. Invest.*, **108**, 189–201.
43. Kasahara, H., Lee, B., Schott, J.J., Benson, D.W., Seidman, J.G., Seidman, C.E. and Izumo, S. (2000) Loss of function and inhibitory effects of human CSX/NKX2.5 homeoprotein mutations associated with congenital heart disease. *J. Clin. Invest.*, **106**, 299–308.
44. Briggs, L.E., Takeda, M., Cuadra, A.E., Wakimoto, H., Marks, M.H., Walker, A.J., Seki, T., Oh, S.P., Lu, J.T., Sumners, C. *et al.* (2008) Perinatal loss of Nkx2-5 results in rapid conduction and contraction defects. *Circ. Res.*, **103**, 580–590.